

UV-Patterned Poly(ethylene glycol) Matrix for Microarray Applications

Andréas Larsson, Chun-Xia Du, and Bo Liedberg*

Division of Sensor Science and Molecular Physics, Department of Physics, Chemistry and Biology, Linköping University, SE-581 83 Linköping, Sweden

Received June 26, 2007; Revised Manuscript Received August 14, 2007

A versatile method to fabricate polymeric matrixes for microarray applications is demonstrated. Several different design strategies are presented where a variety of organic films, such as plastic polymers and self-assembled monolayers (SAMs) on planar silica and gold substrates, act as supports for the graft polymerization procedure. An ensemble of poly(ethylene glycol) methacrylate monomers are combined to obtain a matrix with desired properties: low nonspecific binding and easily accessible groups for postimmobilization of ligands. The free radical graft polymerization process occurs under irradiation with UV light in the 254–266 nm range, which offers the possibility to introduce patterns by means of a photomask. The arrays are created on inert and homogeneous coatings prepared either by graft polymerization of a methoxy-terminated PEG–methacrylate or self-assembly of a methoxy-terminated oligo(ethylene glycol) thiol. Carboxylic acid groups, introduced in the array spots either during graft polymerization or upon wet chemical conversion of hydroxyls, grant the capability to immobilize proteins and other molecules via free amine groups. Immobilization of fluorescent species as well as biotin followed by exposure to a fluorescently labeled antibody directed toward biotin display both excellent integrity of the spots and low nonspecific binding to the surrounding framework. Beside patterns of uniform height and size, an array of spots with varying thickness (a sort of gradient) is demonstrated. Such gradient samples enable us to address critical issues regarding the mechanism(s) behind spatially resolved free radical polymerization of methacrylates. It also offers a convenient route to optimize the matrix properties with respect to thickness, loading capacity, protein diffusion/penetration, and nonspecific binding.

Introduction

Miniaturization and parallelization are crucial methods to employ for the development of more efficient research and diagnostic tools. Such strategies offer faster analysis, smaller sample volumes, and reduced reagent costs, as well as internal referencing and thereby more accurate results. Protein microarrays are valuable complements to DNA/RNA chips, due to the discrepancy often found between messenger RNA expression levels and resulting protein concentrations. Proteins are, however, sensitive to the surrounding conditions, and careful surface design is essential, in order to obtain a robust protein microarray. The surface chemistry should allow immobilization of biomolecules, while preserving their native structure and function, along with a low degree of nonspecific binding. Pioneering work in this field was carried out by MacBeath and Schreiber,¹ who demonstrated immobilization of minute amounts of protein, at high densities, with retained nativity on two-dimensional (2D) surfaces. Via silanization, glass supports were provided with aldehyde groups, which reacted with primary amines on the proteins, and the nonexposed areas were passivated with immobilization of bovine serum albumin (BSA). Zhu and Snyder² compared the above approach with immobilization of hexahistidine-tagged proteins onto nickel-coated glass slides and found that the latter gave superior results. Presumably, the enhanced performance was a result of better orientational control, thus improving the accessibility and presentation of the binding epitopes. In another interesting work, Wacker et al.³ presented a self-assembly process, in which proteins labeled with single-stranded DNA were immobilized in a previously

prepared microarray of complementary DNA sequences. From a commercial perspective, this approach is very attractive since problems related to protein degradation during prolonged storage and transportation are circumvented. The apparent disadvantage is the need for DNA-labeled proteins. On the other hand, the labeling gives control over the protein orientation, as long as it is labeled with care. Recently, Valiokas et al.⁴ prepared an array of spots using functionalized oligo(ethylene glycol)-containing alkyl thiols in self-assembled monolayers (SAMs) on gold. Different relative concentrations of nitrilotriacetic acid (NTA) groups were obtained by mixing thiols, carrying either one or two NTA moieties, with similar thiols lacking NTA. Microdispensing of the thiols was facilitated by a hydrophobic grid (later passivated with BSA), created by microcontact printing. This approach offered a versatile tool for adjusting the affinity for histidine-tagged biomolecules, by varying the molecular valency (i.e., the NTA valency of the thiol) and the surface valency (i.e., the surface concentration of the NTA–thiols), and enabled studies of intricate protein–protein interactions. All these studies employed 2D surfaces, which are not always ideal for protein interactions. To obtain optimal accessibility, the immobilized proteins must be sufficiently separated for steric reasons, which decreases the amount of protein loadable per unit area. One way to increase the loading capacity is to use a three-dimensional (3D) matrix. In a work by Arenkov et al.⁵ acrylamide monomers were graft copolymerized with diacrylates, using 254 nm UV light, onto glass substrates with methacrylate-terminated silane SAMs. An array of 100 μm \times 100 μm pads was prepared, via a photomask, and used to immobilize proteins. In immunoassays, microelectrophoresis was used to promote protein penetration

* Corresponding author. E-mail: bolie@ifm.liu.se.

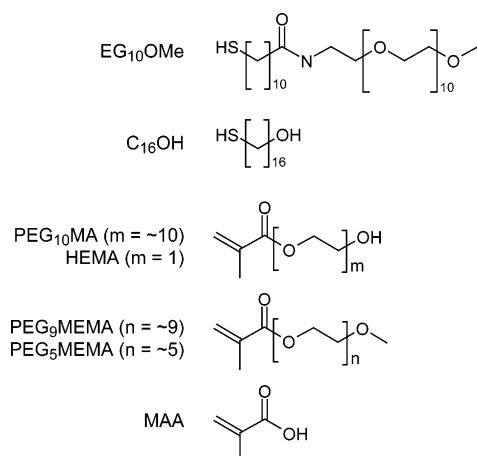


Figure 1. Chemical structures of the two thiols used as grafting platforms and the five methacrylate monomers used in the graft polymerization process.

in the relatively thick (20–40 μm) and cross-linked pads as well as to remove nonspecifically bound proteins.

In the pursuit of a suitable platform for microarrays, poly(ethylene) glycol (PEG) is a component that has been proposed by several groups. Veisheh et al.⁶ reported on an array of 20 $\mu\text{m} \times 20 \mu\text{m}$ gold squares, prepared on silica substrates and subsequently treated with carboxyl-terminated thiols and 5 kDa PEG–silanes. The carboxyl groups in the squares were used for amine coupling, while the PEG-coated silica offered a protein-resistant framework. In another study by Wegner et al.⁷ an amine-terminated SAM on gold was used to immobilize different cysteine-modified peptides in pyridyldithio-functionalized microchannels. The nonexposed areas were back-filled with 2 kDa PEG–*N*-hydroxysuccinimide (NHS) to provide protein-resistant properties. In both these studies, PEG was excluded from the areas in which biomolecular interactions were meant to take place. Biosensor systems based on PEG in a nonpatterned format have been proposed previously,^{8–12} and these studies, along with work from our group,^{13,14} show that this polymer may be used successfully in fabrication of biochips for protein interaction studies.

In the present study, a number of different strategies for designing patterned sensor surfaces are demonstrated. These strategies rely on PEG-containing methacrylates that are graft polymerized onto SAMs or plastic polymers. Self-assembled monolayers based on organosulfur compounds on gold or silanes on silica generally offer excellent grafting platforms, though only the former is discussed here in detail. Two thiols, seen in Figure 1, were employed as grafting platforms. Plastic polymers are also well suited for this purpose, and they can be used as self-supported strips or spin-coated thin films on planar substrates. Supporting planar substrates facilitate examination and are used in this work. Five methacrylate monomers (Figure 1) were graft copolymerized in different constellations. The graft polymerization, previously described in detail,^{13,14} involves a free radical reaction and occurs under irradiation in the 254–266 nm range. The general setup is seen in Figure 2A. The nature of the procedure makes it suitable for generation of gradients and patterns by blocking the incoming irradiation, by means of a slowly moving shutter (Figure 2A) or a photomask (Figure 2B), respectively. The thickness of the matrix is dependent on the time of irradiation,¹³ the power of the light source, and the availability of monomers. Patterns with a thickness up to 170 nm have been observed, although spot thicknesses of 40–60 nm are normally employed in interaction

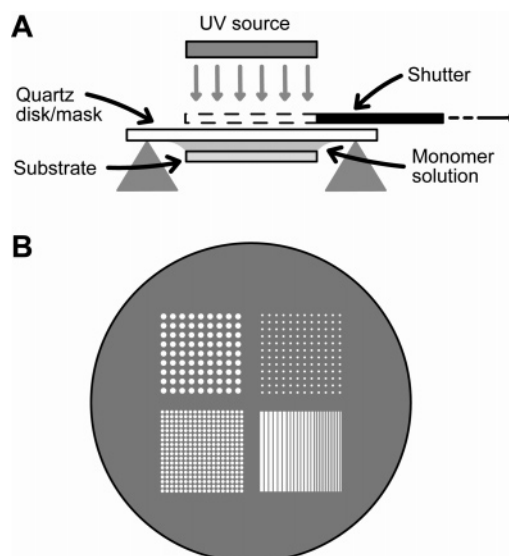


Figure 2. (A) Graphic displaying the sandwich assembly employed during grafting and the shutter, which enables the formation of a gradient. (B) Quartz photomask with different patterns spanning from 5 to 25 μm lines to 20–200 μm spots.

studies. Chemical handles for ligand immobilization are obtained either by using carboxyl-containing monomers, during matrix preparation, or by postcarboxylation of hydroxyl-terminated monomers. These monomers are graft polymerized in array formats on top of inert platforms, and the integrity of the spots is investigated upon immobilization of a fluorescent probe. In addition, the interaction between an immobilized biotin ligand and a fluorescently labeled anti-biotin antibody is examined. Apart from patterns of equal height, a gradient of spots is presented and studied using the same interaction protocol. The patterned surfaces are examined with microscopic wetting, imaging null ellipsometry, atomic force microscopy (AFM), and fluorescence microscopy.

Materials and Methods

Reagents. Hydroxyl-terminated poly(ethylene glycol) methacrylate with an average of 10 ethylene glycol units (PEG₁₀MA), 2-hydroxyethyl methacrylate (HEMA), methoxy-terminated poly(ethylene glycol) methacrylates with an average of 5 and 9 ethylene glycol units (PEG₅MEMA and PEG₉MEMA), methacrylic acid (MAA), bromoacetic acid, *N*-hydroxysuccinimide (NHS), ethanolamine, and dansylcadaverine (DC) were purchased from Sigma-Aldrich Sweden AB. *N*-Ethyl-*N'*-(3-dimethylaminopropyl)carbodiimide (EDC) and HS(CH₂)₁₆OH (C₁₆OH) were obtained from Biacore AB, Uppsala, Sweden, and HS(CH₂)₁₁-CONH(C₂H₄O)₁₁CH₃ (EG₁₀OMe) was obtained from Polypure AS, Norway. 1-Propanol was purchased from Riedel-de Haën. (+)-Biotin-(PEO)₃-amine (BPA) was purchased from Molecular Biosciences, U.S.A. Texas red conjugated rabbit anti-biotin antibody (TRAB) was purchased from Rockland Immunochemicals, U.S.A. The cycloolefin polymer (COP) Zeonor 1020R was obtained as a generous gift from Ämic AB, Uppsala, Sweden.

Substrate Preparation. Silicon (100) wafers (Topsil Semiconductor Materials A/S, Denmark) with a native oxide layer were cut into 12.5 mm \times 12.5 mm pieces and used both with and without gold coating. Prior to evaporation, these substrates were pretreated in a UVO cleaner (model no. 42-220, Jelight Company Inc., U.S.A.) for 4 min. First, a chromium (Cr, Balzers, Liechtenstein, 99.98%) adhesion layer of 25 Å was deposited followed by a gold (Au, Nordic High Vacuum AB, Kullavik, Sweden, 99.99%) layer of 2000 Å. The custom-made evaporation system used was set to work in resistive mode. The evaporation rate was 1–5 Å/s and 10–15 Å/s for chromium and gold,

respectively. The base pressure was on the low 10^{-6} torr scale, whereas the pressure during evaporation was on the high 10^{-6} torr scale.

Photomask Preparation. For the production of PEG matrixes in a patterned format, photomasks consisting of quartz glass disks with chromium patterns on them were used. These photomasks were manufactured through several processing steps in clean-room environment using semiconductor microchip fabrication techniques. More specifically, quartz disks were cleaned using TL-1 (5:1:1 mixture by volume of Milli-Q water (Milli-Q, Millipore, U.S.A.), 30% hydrogen peroxide (Merck KGaA, Germany), and 25% ammonia (Merck KGaA, Germany) for 10 min at 85 °C) and TL-2 (6:1:1 mixture by volume of Milli-Q water, 30% hydrogen peroxide, and 37% hydrogen chloride (Merck KGaA, Germany) for 10 min at 85 °C) procedures before a chromium coating of about 1300 Å was deposited, utilizing the evaporation equipment mentioned above. The quartz/chromium disks were then spin-coated with positive photoresist (Microposit S1818 (Rolm and Haas Electronic Material, U.K.) at 3000 rpm, 30 s). The resulting thickness was about 2 µm. After prebaking for 20 min at 90 °C to evaporate the solvent, the disks were exposed to UV light (6 mW/cm²) through a mother mask in direct contact mode (Karl Süss mask aligner) using an exposure time of 10 s. The mother mask was created with a pattern generator (DWL66 Heidelberg Instruments). The exposed areas were acidified and could be dissolved during the subsequent development step. The alkaline developer (Microposit 351 developer (Rolm and Haas Electronic Material, U.K.)) was mixed with Milli-Q water at a ratio of 1:5 by volume. The developing time was 40–60 s followed by rinsing with Milli-Q water. Hard baking of the resist was then performed for 30 min at 100 °C in order to solidify the remaining photoresist, which later served as a protection layer. At this stage, the patterns had been successfully transferred from the mother mask to the photoresist on the chromium-coated disks. The areas not covered by resist were, thus, unprotected and removed with chromium etching solution (chromium etch, Merck KGaA, Germany). The disks were immersed in the solution for 1–2 min until the patterns were opened up. The residual resist was then stripped from the quartz/chromium disks by 5–10 min of submersion in resist-removal (Microposit remover 1112A (Rolm and Haas Electronic Material, U.K.)) mixed with Milli-Q water at a ratio of 1:1 by volume. Finally, the disks were rinsed in Milli-Q water for 10 min. Thereby the photomasks were ready for grafting experiments.

Grafting and Patterning. The general grafting procedure is described in detail elsewhere,^{13,14} and only a short description is given here. To provide grafting platforms, silica substrates were spin-coated with COP, whereas gold substrates were either spin-coated with COP or coated with thiol SAMs. The two thiols used were C₁₆OH and EG₁₀-OMe (Figure 1). The gold substrates were incubated in 99.5% ethanol (Kemetyl, Haninge, Sweden) thiol solutions of 1 mM for at least 16 h and 100 µM for at least 24 h, respectively. Thereafter, a drop of aqueous monomer solution was placed on the underside of a plain quartz disk or a photomask, which was brought in contact with the sample to form a sandwich assembly in which the sample became *free-hanging* and kept in place by the surface tension of the liquid. The assembly was placed on supports in the reaction chamber, which was purged with nitrogen gas 1 min before and throughout the grafting event. Three different light sources were used: a Philips TUV PL-L 18 W Hg lamp, a Newport Apex light source with a 100 W Hg lamp, and a diode-pumped MBD-266 laser (no nitrogen purging was used in this case). The TUV lamp provided noncollimated light with a distinct emission peak at 254 nm, whereas the Apex provided a collimated output and was used along with a dichroic mirror with main reflectivity at 240–255 nm. In the laser setup, the wavelength was 266 nm and the 0.8 mm diameter beam was expanded with a fused silica lens ($f = 8$ cm) and an aperture of 6 mm was placed in the beam path 10 cm from the sandwich assembly. This arrangement resulted in a beam which was close to collimated, and the total power of the light reaching the sample was about 10 mW. In cases where nonpatterned PEG matrixes were produced, a 1:1 PEG₅MEMA and PEG₉MEMA mixture (PEG-OMe)

in Milli-Q water was used at a total concentration of 240 mM. With the use of the photomasks, patterns were graft polymerized from a 1:1 mixture between PEG₁₀MA and HEMA (PEG-OH) or a 24:23:1 mixture between PEG₁₀MA, HEMA, and MAA (PEG-COOH), both at a total concentration of 240 mM. When grafting spots in a gradient format, a shutter was moved in a stepwise manner, revealing another row of spots every 30 s, during 6 min of irradiation with the TUV lamp. The preparation of nonpatterned gradients has been reported on before.¹⁴ After each grafting step, the samples were ultrasonicated for 5 min in ethanol and dried in nitrogen gas.

Matrix Carboxylation, Immobilization, and Interaction. To carboxylate arrays of PEG-OH matrix, the samples were incubated in an aqueous solution of 1 M bromoacetic acid and 2 M sodium hydroxide for 16 h at room temperature during shaking.¹⁵ After activation of the carboxyl groups (both PEG-COOH and carboxylated PEG-OH) for 20–30 min with an aqueous mixture of EDC and NHS at 0.2 and 0.05 M, respectively, ligands were immobilized via amine coupling onto the spots during 60 min of incubation. The matrix was then deactivated with an aqueous solution of 1 M ethanolamine during 60 min. Dansyl cadaverine was immobilized at 0.1 mM in 1-propanol, and BPA was immobilized at 0.1 mM in Milli-Q water. Samples with immobilized BPA were subsequently incubated in 700 nM TRAB in HBS-EP (10 mM Hepes, 0.15 M NaCl, 3 mM EDTA, 0.005% polysorbate 20, pH 7.4) for 60 min. The samples were rinsed and dried after each step.

Fluorescence Microscopy. Microphotographs of samples with fluorescent probes were recorded in dry state using an epifluorescence microscope (Zeiss Axiovert inverted microscope A200 Mot) equipped with a charge coupled device (CCD) camera (Axiocam HRC, three chip). A 10× magnification objective was used along with 405/15 and 546/12 nm excitation filters for measurements on DC and TRAB, respectively.

Imaging Null Ellipsometry. The ellipsometry images of patterned surfaces were acquired using a Nanofilm EP³-SE imaging null ellipsometer (Nanofilm Technologie, Germany). A laser beam with a wavelength of 532 nm was used along with a 5× magnification objective and a beam expander for the silica substrate, whereas for the gold substrate, a wavelength of 831 nm was selected from the output of a Xe lamp with an interference filter and a 2× magnification objective was used. In both cases, the angle of incidence was set at 60° and the refractive index of all organic material on the surface was assumed to be 1.5.

Atomic Force Microscopy. Topographical images of patterned samples in their dry state were obtained using an EnviroScope atomic force microscope (Digital Instruments, U.S.A.) run in contact mode with a DNP-S tip (Veeco, U.S.A.).

Microscopic Wetting. Condensation of water from the surrounding atmosphere to reveal the matrix spots was induced by cooling the substrate to a temperature close to the dew point with a Peltier element. The wettability patterns were inspected with an Olympus zoom stereo light microscope SZ60 connected to an Olympus E-300 digital camera for image capturing.

Results and Discussion

Patterning Capabilities. The versatility of the presented strategies for preparation of patterned surfaces and subsequent immobilization of ligands are summarized in Figure 3. Pathway I is well suited for sensor applications provided that the SAM possesses protein-resistant properties. The SAM used herein consists of oligo(ethylene glycol) (OEG)-functionalized alkyl thiols which are known to have excellent protein-resistant properties.¹⁶ Route a presupposes a matrix with available hydroxyl groups, for carboxylation with bromoacetic acid,¹⁵ in the patterned areas and the absence of them in the surrounding areas. When combining pathway I and route a it is therefore crucial to avoid hydroxyl-terminated SAMs. In route b, a carboxyl-containing matrix is obtained by including a carboxy-

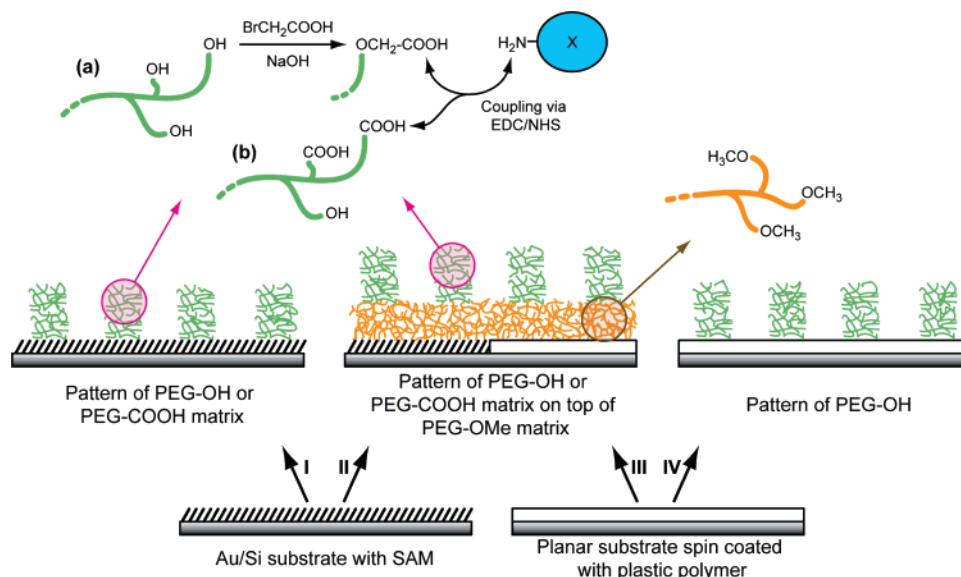


Figure 3. Schematic illustration of different approaches used to prepare patterned surfaces. Pathway I employs a SAM which is required to display protein-resistant properties, for example, an OEG-functionalized monolayer. In pathways II and III, a hydroxyl-terminated alkylthiol SAM and a thin plastic polymer film are used as grafting platforms, respectively. The pathways II and III are less dependent on the properties of the grafting platforms, since they are covered by a PEG-OMe matrix, as long as they support efficient graft polymerization. Carboxyl groups, which may be used for ligand immobilization, are obtained either by route a, treatment with bromoacetic acid, or route b, use of carboxyl-containing monomers. Pathway IV is also based on a plastic polymer grafting platform. The nonpatterned parts of the polymer need to be passivated in some way, e.g., with BSA, to avoid nonspecific binding of ligand as well as analyte proteins to the polymer surface.

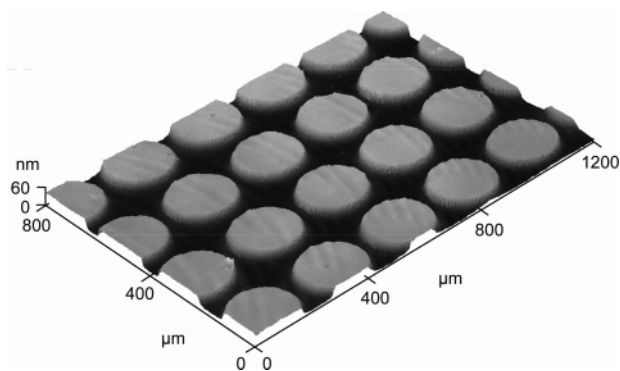


Figure 4. Ellipsometry image of a silica substrate spin-coated with COP and patterned with 200 μm PEG-OH matrix spots spaced by 50 μm (pathway IV in Figure 3) using the MBD laser.

lated monomer during polymerization, making the postcarboxylation step redundant. In addition, it is no longer necessary to impose the restrictions, mentioned above, on the use of terminal hydroxyl groups of the SAM. Pathways II and III are less dependent on the properties of the grafting platform as long as it supports efficient graft polymerization. When the patterned areas are postcarboxylated, using route a, a methoxy-terminated PEG matrix is used as the underlying matrix to avoid unwanted carboxylation and obtain protein resistance. In order to use pathway IV for sensor applications it is necessary to further modify the exposed plastic polymer surface to prevent nonspecific binding, e.g., via back-filling with serum albumin. Combinations of these strategies lead to a wide range of different patterns, and all of them cannot be covered here. Instead, a selection of patterned surfaces is shown and discussed. Figure 4 displays an imaging null ellipsometry recording of a silica substrate, which followed pathway IV and was patterned with 200 μm PEG-OH matrix spots separated by 50 μm using the MBD laser during 8 min of irradiation. The laser setup does not offer proper collimated light but still gives sharper features than the noncollimated from the TUV lamp. The fact that the slightly longer wavelength of the laser (266 nm), compared to

that of the normally used light sources (254 nm), also supported the graft polymerization process was an interesting observation. Figure 5A shows an AFM image of a 100 μm PEG-OH spot that was graft polymerized on top of a nonpatterned PEG-OMe matrix, in turn prepared on a silica substrate, via pathway III. In both steps an irradiation time of 8 min with the TUV lamp was used. Despite the noncollimated light source, spots prepared in this manner display surprisingly well-defined and sharp edges. However, with collimated light, provided by a unit such as the Apex, the pattern size can be reduced to reach the low-micrometer range. The sample in Figure 5B was also prepared on a silica substrate but patterned without an intermediate matrix layer (pathway IV). The PEG-OH patterns (20 μm spots separated by 20 μm) were prepared with the Apex light source during 10 min of irradiation. Presented in Figure 5C is an assembly of AFM images of a series of line structures, prepared using the same parameters used for the previous sample. Adjacent to each image, the corresponding thickness profile is given. It is interesting to note the different shapes of the structures when going from 200–100 to 25–5 μm . In case of the smaller patterns, the edges are more pronounced and constitute the tallest parts of the structures, whereas a more uniform thickness is observed for the larger patterns. The reason for this occurrence is unclear, though a plausible explanation is that the output power of the Apex is higher than that of the laser and the TUV lamp and therefore speeds up the propagation of polymerization leading to a higher rate of monomer consumption. For instance, at the rim of a spot there is less competition for monomers because of a steady inward flow of monomers from the top as well as from the surroundings (nonilluminated parts) resulting in a more efficient grafting in these regions, compared to the center of the spot. Put otherwise, the supply of monomers may be diffusion limited at the seemingly higher polymerization rate obtained when using the Apex light source.

Moreover, it has been found that a number of different thiol and silane SAMs and plastics support the graft polymerization method presented herein.¹⁷ One important observation, however,

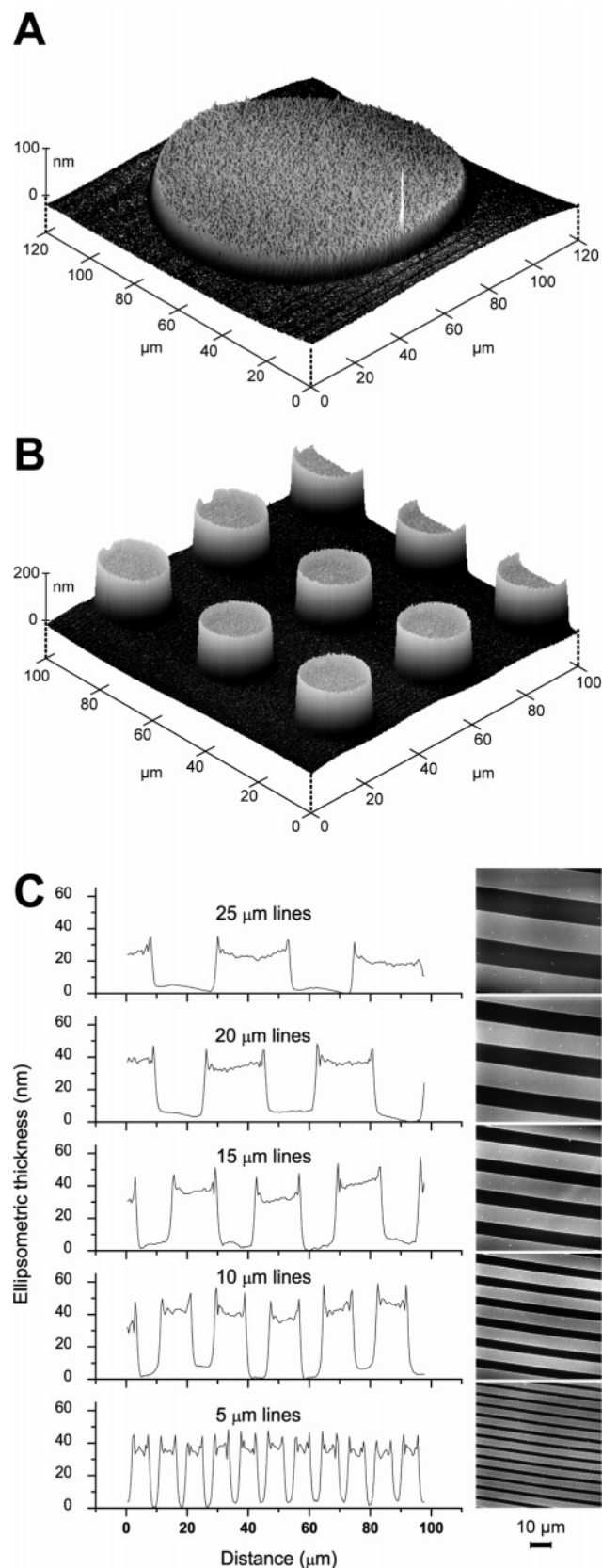


Figure 5. Atomic force microscopy images of silica substrates where different graft polymerization approaches from Figure 3 have been used. (A) Underlying matrix of PEG-OMe and a $100\ \mu\text{m}$ PEG-OH spot on top (pathway III), both graft polymerized with the TUV lamp. (B) PEG-OH spots, $20\ \mu\text{m}$ in size, spaced by $20\ \mu\text{m}$ (pathway IV) using the Apex light source. (C) Series of lines along with their respective thickness profiles. The PEG-OH lines are 5, 10, 15, 20, and $25\ \mu\text{m}$ wide and spaced with equal distances, and they were prepared via pathway IV using the Apex light source.

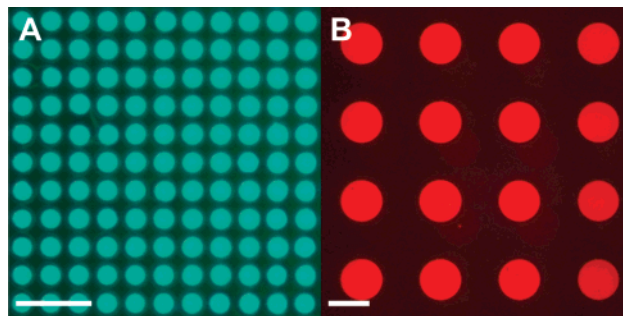


Figure 6. Fluorescence microphotographs showing different preparation strategies from Figure 3 on gold substrates. The scale bars correspond to $100\ \mu\text{m}$. (A) Homogeneous PEG-OMe matrix patterned with PEG-OH $20\ \mu\text{m}$ spots, spaced by $20\ \mu\text{m}$, following pathway III and route a. Dansyl cadaverine was immobilized in the carboxylated spots, and the image acquisition time was 300 ms. (B) Homogeneous PEG-OMe matrix graft polymerized onto a C_{16}OH SAM and patterned with $100\ \mu\text{m}$ PEG-COOH, spaced by $100\ \mu\text{m}$, following pathway II and route b. (+)-Biotin-(PEO)₃-amine was immobilized in the spots, and the sample was subsequently exposed to TRAB. The image acquisition time was 600 ms.

is that very hydrophobic surfaces, such as those formed by methyl-terminated alkyl thiols, are not suitable. This is most likely a consequence of poor wetting of the surface and, thus, insufficient contact between the monomer solution and the organic grafting platform.

Pattern Integrity and Biospecific Interactions. To investigate the integrity of the patterns, pathways II and III were explored using gold as the supporting substrate. In the latter case, the underlying and homogeneous PEG-OMe matrix was graft polymerized on spin-coated COP by 10 min of irradiation with the TUV lamp, and the $20\ \mu\text{m}$ PEG-OH patterns separated by $20\ \mu\text{m}$ were prepared by 10 min of irradiation with the Apex lamp. Thereafter, carboxylation following route a was carried out, and after activation with EDC/NHS, the surface was incubated in a solution of DC. Analysis with epifluorescence microscopy showed distinct fluorescent spots and thus confirmed a successful design strategy, where the spots could be selectively activated (Figure 6A). In the other case, a SAM of C_{16}OH was used as the supporting substrate for a PEG-OMe matrix, which was graft polymerized during 6 min of irradiation from the TUV lamp. Route b was followed, and PEG-COOH spots with a diameter of $100\ \mu\text{m}$ and separated by $100\ \mu\text{m}$ were prepared during 4 min of irradiation with the TUV lamp. The BPA ligand was then immobilized using EDC/NHS-assisted amine coupling. After exposure to TRAB, the sample was examined. As seen in Figure 6B, this design strategy also enables the creation of distinct spots, which permit spatially selective immobilization and biospecific interactions to take place. The use of the carboxylated MAA in this approach eliminates the need of the time-consuming postcarboxylation process. However, direct immobilization of large molecules, such as proteins, works poorly in MAA-based matrixes most likely because of steric constraints and/or a nonideal key-lock binding situation. Thus, an ethylene glycol (EG) spacer arm, like the one in BPA, might be needed to aid efficient immobilization of proteins. This matter is further discussed below. Ideally, a precarboxylated monomer with a built-in spacer should therefore be used, as it would not only save time, but also offer the possibility to fine-tune and optimize the content of carboxyl groups in the matrix.

An interesting alternative to prepare patterned PEG sensor matrixes was recently presented by Textor and co-workers.^{18–22} Different patterns in the low-micrometer domain were created by adsorption of PEG-graft-poly(L-lysine) (PEG-g-PLL), func-

tionalized with either biotin^{18,19} or NTA,²⁰ onto niobium oxide substrates using molecular assembly patterning by lift-off (MAPL), followed by back-filling of nonfunctionalized PEG-g-PLL. These approaches give opportunities for capturing biomolecules, using biotin labels (and streptavidin) and histidine tags, respectively. In these reports, however, linear PEG chains are end-point attached to the surface thus providing, at maximum, one functional group per grafting site (PEG chain) for immobilization. An inherited drawback of this design is that it limits the number of available immobilization sites for the ligand and thereby the attainable response upon analyte binding. The presented PEG matrix, on the other hand, has the potential of providing a large number of functional groups (e.g., COOH) per grafting site and thereby an increased response (given that the matrix is permeable to the molecules of interest). It should be remembered, however, that in kinetic measurements a small amount of immobilized ligand is desirable in order to minimize mass transport limitations, in which case the linear PEG approach may be considered advantageous over the branched methacrylate coatings discussed herein.

In contrast to methods based on adsorption of PEG-g-PLL,²¹ which are dependent on a negatively charged surface (normally metal oxides), the present graft polymerization method is very versatile and is applicable to many different substrates. Moreover, the electrostatic interaction between PEG-g-PLL and the negative surface is disrupted by high ionic strengths and extreme pH values. Though recent advances in the field have circumvented this issue by enabling covalent anchoring of the copolymer, this route adds further restrictions in the choice of substrate by demanding an aldehyde-presenting surface.²²

Gradient of Spots. By investigation of microarrays in a gradient format, issues regarding the grafting mechanism and protein permeability of the PEG matrix may be addressed. Optimization of spot thickness also offers a means of adjusting the level of the output signal to suit different combinations of read-out techniques and molecular interactions. It is well-known in the area of protein microarraying that large variations in molecular size of the analyte and/or affinities to the ligand make high demands on the dynamic range of the transducer technique used to read the microarray. A gradient of spots might be a convenient route to meet these demands (i.e., more efficiently utilize the dynamic range of the setup) by accommodating ligands for large analytes/high-affinity interactions in thin (low capacity) spots and ligands for small analytes/low-affinity interactions in thick (high capacity) spots.

Gradients of PEG matrix spots were prepared using pathway I and further processed via route a. The SAM used consisted of EG₁₀OMe, and the spots were 200 μm in diameter and separated by 100 μm . In Figure 7, the same set of spots is imaged with three different techniques: microscopic wetting, fluorescence microscopy, and imaging null ellipsometry. The wetting image (Figure 7A) was taken before carboxylation, while the two other pictures were acquired after carboxylation, immobilization of BPA, and exposure to TRAB (fluorescence microscopy, Figure 7B, and imaging null ellipsometry, Figure 7C). As seen, the first proper sign of graft polymerization on the surface is discerned for spots that have been irradiated for 3 min. This behavior is puzzling, considering previous findings where rapid matrix growth was observed the first couple of minutes.¹³ However, it may be explained by diffusion of interfering species, such as inhibitors (present in the monomer stock solutions) and oxygen, from the area still covered by the shutter. In other words, there may be a start-up phase in which these species are consumed before the actual graft polymerization begins. This

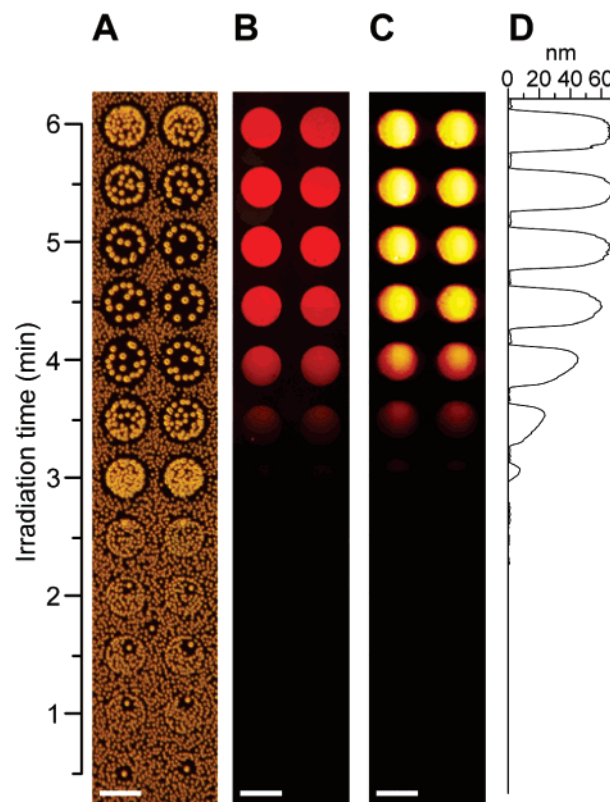


Figure 7. Images and thickness profile of a gradient of 200 μm PEG-OH matrix spots spaced by 100 μm on an EG₁₀OMe SAM (pathway I in Figure 3). Spots were irradiated for up to 6 min with 30 s increments. The spots are the same ones in all cases. The scale bars correspond to 200 μm . (A) Wetting image before carboxylation. (B) Fluorescence microphotograph after carboxylation, immobilization of BPA (route a), and interaction with TRAB. The image acquisition time was 75 ms. (C) Ellipsometry image after the same treatment as in (B). (D) Thickness profile of the image in C.

possibility is supported by the sloping appearance of the spots found at 3–4 min of irradiation. The part of the spots facing the area which experienced longer exposure to the UV light displays more efficient grafting than the part facing the area that was irradiated for a shorter period of time. This behavior is particularly obvious in the thickness profile in Figure 7D. In other words, it is suggested that the monomer solution covered by the shutter acts as a reservoir of interfering species which may diffuse into the exposed areas and reduce the grafting efficiency. In such case, removal or consumption of the interfering species prior to polymerization would eliminate these effects. An inhibitor removal kit may prove useful or possibly a brief period of irradiation of the whole monomer solution before grafting with the photomask. Furthermore, as long as the thickness increases, the intensity of the fluorescence emission seems to increase as well. It was previously found that immobilization of proteins in the same kind of matrix, but in a thickness gradient format, was somehow hindered from penetrating the thick regions of the matrix properly.¹⁴ It is difficult to reach any conclusions regarding the penetrating capability of TRAB during interaction with the immobilized BPA, based on the data presented here. However, it is not unlikely that the bivalent interaction between TRAB and BPA, as opposed to the case of the amine coupling which renders the possibility for multiple attachment points in the highly carboxylated matrix,¹⁴ promotes the penetration. The amine coupling protocol is in fact believed to effectively cross-link the present matrix upon immobilization of large biomolecules, thus preventing further protein penetration.^{13,14} To circumvent this problem, it

is suggested that future immobilization in this matrix should employ protocols that involves single-point attachment. Suitable examples include immobilization of appropriate ligands labeled with a thiol (e.g., a cysteine residue), biotin, or histidine tag. The relatively small swelling ($\sim 30\%$) found in AFM measurements, upon hydration of a matrix with a dry thickness of about 370 Å (route IV, data not shown), may indicate that the matrix itself is fairly dense with a certain level of cross-links, which could be a contributing factor to the restricted protein penetration. To further elucidate the properties of the matrix in this respect, real-time measurements on immobilization and subsequent interactions in gradients of spots are currently being undertaken and will be reported on shortly. Alternatively, the seemingly small pore size may be exploited in a similar manner as was done by Yadavalli et al.,²³ who graft copolymerized PEG–diacrylates and NHS–PEG–acrylates onto a methacrylate-terminated silane SAM on silica and glass in the presence of initiators and enzymes. With the use of either a mask or micro spotting pins, a 365 nm UV light source was used to create a PEG hydrogel with captured enzymes. Though suitable for low molecular mass analytes, such as the corresponding enzyme substrates, the very small mesh size (~ 9 Å) reported and the lack of protein-resistant properties in the surrounding framework make this approach less useful for studies of protein–protein interactions.

When comparing the acquisition time for the fluorescence microscopy images seen in Figures 6B (route b) and 7B (route a), it is seen that the acquisition time is 8 times longer, signifying smaller amount of TRAB, in the former case. This occurrence might be a consequence of an altered structure with a smaller pore size due to the presence of MAA. Alternatively, it indicates that the spacer arm of BPA is not long enough to make the biotin moiety accessible to TRAB in an optimal fashion when MAA is used to obtain the carboxyl groups. Differences in the amount of carboxyl groups could make such a comparison difficult, but infrared reflection absorption recordings revealed comparable carboxylation levels (data not shown). The length of the spacer is obviously a crucial factor in this context since the ligand must reach the interaction site, which might be buried in the interior of the analyte. It should be noted that an EG spacer is not always the ideal choice and, for example, alkyl or oligoglycine may be more suitable, depending on the polar/apolar character of the binding pocket. For instance, in studies on the interaction between benzenesulfonamide ligands and carbonic anhydrase II an alkyl spacer was found to work better than both EG and oligoglycine spacers of similar length.^{24,25}

Conclusions

A functional matrix, combining the possibility to immobilize ligands in designated areas along with low nonspecific binding of proteins, has been developed for microarray applications. Patterns like arrays of spots and lines in the size range of 5–200 μm have been produced. By means of microdispensing, different ligands may be immobilized in different spots thereby realizing a very useful microarray chip. The thickness of the spots in such an array is normally kept around 40–60 nm, although thicknesses up to 170 nm have been observed. The fact that the surrounding inert framework is not activated prior to immobilization makes the dispensing procedure trouble-free, since excess ligand solution, accidentally deposited in the framework areas, is simply rinsed away. In addition, the higher hydrophilicity in the spots further aids dispensing by reproving misdirected drops to a certain extent. The present study is

restricted to the use of COP and thiol SAMs as grafting platforms, though similar results are obtained using other plastic polymers and silane SAMs on silica and glass. Such flexibility in the use of substrate is rare and considered to be a great advantage, making this approach suitable in many instances. The possibility to incorporate a variable amount of carboxyl groups further extends its adaptability, and the fact that a branched structure of PEG chains is produced increases the availability of chemical handles for immobilization, compared to sensor devices based on linear PEGs.

Taken together, a versatile method of producing arrays of PEG spots in which ligands are conveniently immobilized, assisted by an inert EG framework, has been demonstrated. The PEG-based matrix supports biospecific interactions, though more work is needed to improve the permeability for large and structurally complex biomacromolecules. In addition, efforts have been made to gain better insight into the factors that govern the growth of the matrix in a patterned format and the impact of interfering species, which may include inhibitors and oxygen. Such investigations were aided by gradients of spots, which might also be used in process optimizations as well as for protein microarrays capable of monitoring many parallel interactions with very different response levels.

Acknowledgment. This work was supported by the Swedish Research Council (VR) and the Foundation for Strategic Research (SSF) through the Biomimetic Materials Science Program.

References and Notes

- (1) MacBeath, G.; Schreiber, S. L. *Science* **2000**, *289*, 1760–1763.
- (2) Zhu, H.; Snyder, M. *Curr. Opin. Chem. Biol.* **2003**, *7*, 55–63.
- (3) Wacker, R.; Schröder, H.; Niemeyer, C. M. *Anal. Biochem.* **2004**, *330*, 281–287.
- (4) Valiokas, R.; Klenkar, G.; Tinazli, A.; Tampé, R.; Liedberg, B.; Piehler, J. *ChemBioChem* **2006**, *7*, 1325–1329.
- (5) Arenkov, P.; Kukhtin, A.; Gemmell, A.; Voloshchuk, S.; Chupeeva, V.; Mirzabekov, A. *Anal. Biochem.* **2000**, *278*, 123–131.
- (6) Veishe, M.; Zareie, M. H.; Zhang, M. *Langmuir* **2002**, *18*, 6671–6678.
- (7) Wegner, G. J.; Wark, A. W.; Lee, H. J.; Codner, E.; Saeki, T.; Fang, S.; Corn, R. M. *Anal. Chem.* **2004**, *76*, 5677–5684.
- (8) Piehler, J.; Brecht, A.; Valiokas, R.; Liedberg, B.; Gauglitz, G. *Biosens. Bioelectron.* **2000**, *15*, 473–481.
- (9) Huang, N.-P.; Vörös, J.; De Paul, S. M.; Textor, M.; Spencer, N. D. *Langmuir* **2002**, *18*, 220–230.
- (10) Masson, J.-F.; Battaglia, T. M.; Kim, Y.-C.; Prakash, A.; Beaudoin, S.; Booksh, K. S. *Talanta* **2004**, *64*, 716–725.
- (11) Muñoz, E. M.; Yu, H.; Hallock, J.; Edens, R. E.; Linhardt, R. J. *Anal. Biochem.* **2005**, *343*, 176–178.
- (12) Lata, S.; Piehler, J. *Anal. Chem.* **2005**, *77*, 1096–1105.
- (13) Larsson, A.; Ekblad, T.; Andersson, O.; Liedberg, B. *Biomacromolecules* **2007**, *8*, 287–295.
- (14) Larsson, A.; Liedberg, B. *Langmuir*, accepted for publication, 2007.
- (15) Löfås, S.; Johnsson, B. *J. Chem. Soc., Chem. Commun.* **1990**, 1526–1528.
- (16) Harder, P.; Grunze, M.; Dahint, R.; Whitesides, G. M.; Laibinis, P. E. *J. Phys. Chem. B* **1998**, *102*, 426–436.
- (17) Within our group, the thiols $\text{HS}(\text{CH}_2)_{16}\text{OH}$, $\text{HS}(\text{CH}_2)_{15}\text{COOH}$, $\text{HS}(\text{CH}_2)_{11}\text{CONH}(\text{C}_2\text{H}_4\text{O})_{11}\text{CH}_3$, $\text{HS}(\text{CH}_2)_2(\text{C}_2\text{H}_4\text{O})_6\text{OCH}_3$, and $\text{HS}(\text{CH}_2)_{15}\text{CONH}(\text{C}_2\text{H}_4\text{O})_4(\text{CH}_2)_2\text{NHCOCH}_2\text{C}_6\text{H}_5(\text{NO}_2)_2$ on gold and the silanes (3-aminopropyl)triethoxysilane and 3-methacryloxypropyltrimethoxysilane on silica and glass have been used as grafting platforms. In addition, the plastic polymers polyethylene, poly(methyl methacrylate), cycloolefin polymer, and polystyrene have been used as self-supported platforms. The latter two have also been used as spin-coated films on gold, silica, and glass.
- (18) Falconnet, D.; Pasqui, D.; Park, S.; Eckert, R.; Schiff, H.; Gobrecht, J.; Barbucci, R.; Textor, M. *Nano Lett.* **2004**, *4*, 1909–1914.
- (19) Falconnet, D.; Koenig, A.; Assi, F.; Textor, M. *Adv. Funct. Mater.* **2004**, *14*, 749–756.

- (20) Zhen, G.; Falconnet, D.; Kuennemann, E.; Vörös, J.; Spencer, N. D.; Textor, M.; Zürcher, S. *Adv. Funct. Mater.* **2006**, *16*, 243–251.
- (21) Kenausis, G. L.; Vörös, J.; Elbert, D. L.; Huang, N.; Hofer, R.; Ruiz-Taylor, L.; Textor, M.; Hubbell, J. A.; Spencer, N. D. *J. Phys. Chem. B* **2000**, *104*, 3298–3309.
- (22) Blättler, T. M.; Pasche, S.; Textor, M.; Griesser, H. J. *Langmuir* **2006**, *22*, 5760–5769.
- (23) Yadavalli, V. K.; Koh, W.-G.; Lazur, G. J.; Pishko, M. V. *Sens. Actuators, B* **2004**, *97*, 290–297.
- (24) King, R. W.; Burgen, A. S. V. *Proc. R. Soc. London, Ser. B* **1976**, *193*, 107–125.
- (25) Jain, A.; Huang, S. G.; Whitesides, G. M. *J. Am. Chem. Soc.* **1994**, *116*, 5057–5062.

BM700707S